Electronic properties of (111) twin boundaries and twinning superlattices in lead sulfide

Z. Ikonic, G. P. Srivastava, and J. C. Inkson
Department of Physics, Exeter University, Stocker Road, Exeter, EX4 4QL, United Kingdom
(Received 24 March 1995)

The electronic properties of single twin boundaries in lead sulfide, and of superlattices based upon them, are calculated and discussed. Substantial differences are noted from a similar study based on zinc-blende-type semiconductors. It is found that such superlattices can have either wider or narrower band gaps than the homogeneous material.

Twin boundaries and related structures (stacking faults) are among the most common type of defects in semiconductors. The two sides of a twinned crystal may be viewed as being rotated with respect to each other, and joined at some crystal plane. In face-centered-cubic crystals the (111) plane is the most frequently occurring twinning plane, and the two halves of the crystal on either side of the boundary are rotated by 180° (or 60°) about the [111] axis. These defects usually appear unintentionally, e.g., due to strain, and may have a significant influence on semiconductor electronic properties, acting, e.g., as scattering centers and lowering the electron mobility, or as recombination centers, etc. The electronic properties of twinning boundaries have been almost exclusively studied for zinc-blende-type semiconductors, since the vast majority of important semiconductors crystallize in this fashion. However, twinning appears in other crystal systems as well.[1]

In this paper we consider the electronic properties of twin boundaries in the important small-band-gap rocksalt-type semiconductor PbS. Twinning is commonly found[2] in naturally occurring mineral PbS, *galena*. Growth twins are normally of (111) type, but other twinning planes, most prominent being (113), also occur, presumably due to stress to which galena is subjected. In laboratory-grown bulk PbS single crystals, twinning has not been reported as a problem, even when starting from natural galena raw material.[3] However, the (111) twinning in PbS has been reported during dendritic growth.[4] Similar to the zinc-blende case, twinning in rocksalt crystals may be viewed as a reversal of the atomic stacking sequence along the [111] axis. However, there is a significant difference in the structure of twins based on zinc-blende- and rocksalt-type crystals. In the former the twinning plane, where the stacking reversal takes place, lies in between the two atoms joined by [111]-directed bonds, and the junction of the two crystal halves is highly perfect in the sense that all the bond lengths and angles are preserved. In case of rocksalt-type crystals, the twinning plane contains atoms, as depicted in Fig. 1, and the junction is "less perfect" because only the bond lengths are preserved; bond angles are not. In such a situation, some amount of interface reconstruction may be expected to take place, but this will probably not be a large effect, since bond lengths are much more important than bond angles for the total energy of the structure.

Two types of twins may exist, anionic or cationic, depending on which type of atoms occupy the twinning plane. We are not aware of any study, experimental or theoretical, to determine which type of twins (if not both) actually occurs in PbS. In the somewhat related case of AgBr, also a rocksalt-type material where twinned microcrystals appear and are considered advantageous for the photographic recording process, atomistic simulations have indicated that anionic twins are somewhat more stable than cationic ones.[5] We do not know whether this is the case for PbS, so we have done the calculations for both cases. The same study for AgBr also indicated that the reconstruction in the vicinity of the interface is rather small, and the same may be expected for PbS, so this effect may be neglected to a first approximation.

The electronic properties of single twin boundaries in PbS are first analyzed. We then calculate and discuss the electronic properties of twinning superlattices, a possible structure based on this type of defects, that we have recently proposed and studied for the case of zinc-blende-type semiconductors.[6,7]

Lead sulfide is an L-type direct-band-gap semiconduc-

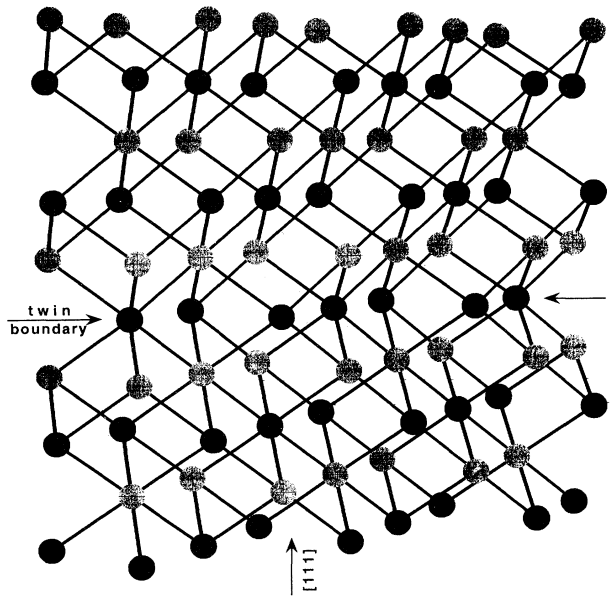

FIG. 1. The structure of PbS crystal in the vicinity of a twin boundary. Light and dark atoms may denote either of Pb and S atoms.

tor, with the extrema of both the conduction and valence bands occurring at the exact L point. The band gap is 0.287 eV at low temperatures. Band energies at all other Brillouin-zone symmetry points (e.g., Γ and X) are very far (a few eV) from the band edges at L. The method used in our calculations is an empirical pseudopotential-based layer method. Used for finding the electronic structure of either superlattices or single twins, this is not a supercell-type method. It considers individual layers of the superlattice as slabs of bulk semiconductors, with their own complex band structures. These are calculated and used to propagate the wave function across the superlattice period. The details are described in our previous publications.[7-9] We may note that, in spite of its relative simplicity, the results of this method for zinc-blende twins compare favorably to those obtained by more sophisticated *ab initio* self-consistent calculations. The pseudopotential form factors for PbS are taken from Ref. 10. The spin-orbit coupling is important and therefore taken into account. However, its role is quite different here than in zinc-blende semiconductors. It leaves the valence and conduction bands doubly degenerate (it is only some higher and lower bands that get split), but influences the band gap and effective masses, making the L valleys more spherical.[11] A total of 31 in-plane Fourier components ($\mathbf{g}_{\parallel}$ values) were used in interface matching, corresponding to a total of 89 three-dimensional reciprocal lattice vectors, up to and including the (331) star.

In order to discuss the electronic properties of twin boundaries and superlattices, we note that two out of eight L points project onto the $\bar{\Gamma}$ (center), and the other six onto six $\bar{M}$ (edge) points of the interface Brillouin zone (Fig. 2). Therefore, the low-energy electronic structure, of importance for transport and optical properties, should be explored in the vicinity of these two points. The physics of electron behavior at the twinning boundaries is also discussed at length in our previous paper.[7] In brief, the nontrivial electronic properties stem from the fact that the wave functions at any point of the interface Brillouin zone are rotation sensitive, and the same

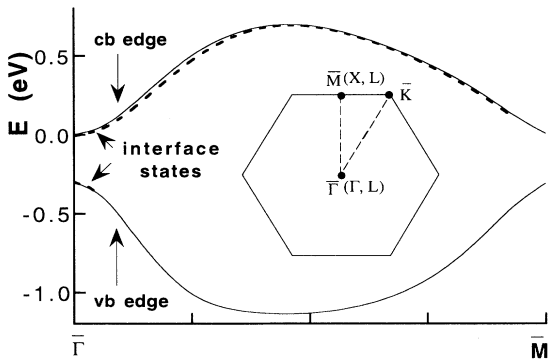

FIG. 2. The projected band structure of PbS (solid lines), and interface bound states (dashed lines, for the case of anionic twin interface only) along the $\bar{\Gamma}$-$\bar{M}$ line of the interface Brillouin zone. The insert displays the (111) interface Brillouin zone, with mapping of some points of the bulk Brillouin zone. (The $\bar{M}$ point is at $|\mathbf{k}_{\parallel}| = 0.8165 \times 2\pi/a$ away from the $\bar{\Gamma}$ point.)

applies to the dispersion along the [111] direction (except at the exact $\bar{\Gamma}$ point). This implies a considerable scattering of carriers at the twinning boundary, resulting in a limited transmission probability through the interface, and may also result in the appearance of interface bound states.

For both anion- and cation-type twin boundaries we have searched for interface bound states along the $\bar{\Gamma}-\bar{M}$ line of the interface Brillouin zone. Bound states are found only when the interface plane contains anion (sulphur) atoms. These lie slightly above the valence-band top or below the conduction-band bottom. The conduction-band-related interface state could be traced from $\bar{\Gamma}$ almost up to $\bar{M}$ point (Fig. 2). It is approximately 8 meV below the local conduction-band edge, and is weakly localized, with its wave-function amplitude decay constant being just 0.04 per crystal unit cell (i.e., it is extended over approximately 20 unit cells). The valence-band-related interface state was found in a rather narrow range of the in-plane wave-vector ($\mathbf{k}_{\parallel}$) values close to the $\bar{\Gamma}$ point, and is only 3 meV above the valence-band edge, and is even less localized.

In calculating the electron (hole) transmission through the twin boundary, the incident state energies were taken in a limited range, starting from the conduction- (valence-) band edge, up to 300 meV above (below) it, to cover the range that thermal or hot electrons (holes) may acquire. The results for the transmission at or close to $\bar{\Gamma}$ and $\bar{M}$ interface Brillouin-zone points are given in Fig. 3. The transmission is different for the two types of interfaces, especially at the $\bar{M}$ point, and also has a non-negligible variation with $\mathbf{k}_{\parallel}$. In both interfaces the low-energy carriers experience considerable scattering at the twin interface, which would adversely influence their mobility.

Finally, in Fig. 4 we present some results for PbS-based twinning superlattices. Calculations were again performed for the $\bar{M}$ and $\bar{\Gamma}$ points of the interface Brillouin zone, where the low-energy part of the miniband spectrum occurs. Although one may imagine superlattices with both types of interfaces present, here we consider the simpler cases of all-cationic or all-anionic interfaces. With this restriction one may generally have m and n monolayers of reversely oriented material per period, denoted as (m,n) superlattice. The thickness of one monolayer is $a/\sqrt{3} = 0.343$ nm (a is the cubic lattice constant). Here we display the results for the symmetric (n,n) superlattices only.

Just as the transmission and the existence of bound states depend on the type of interface, so does the miniband structure of the superlattice. Scattering at the interfaces is clearly quite sufficient to induce considerable minigaps, though these are usually narrower than the width of allowed minibands. The feature common to superlattices of both anionic and cationic types is that the minibands are rather broad for thin-period ($n = 5-8$) superlattices, which is due to rather small values of electron and hole effective masses (~ 0.1 of the free-electron mass). The important effect here, except for miniband formation, is that the band gap is remarkably different from its bulk value. Weakly localized bound states at the

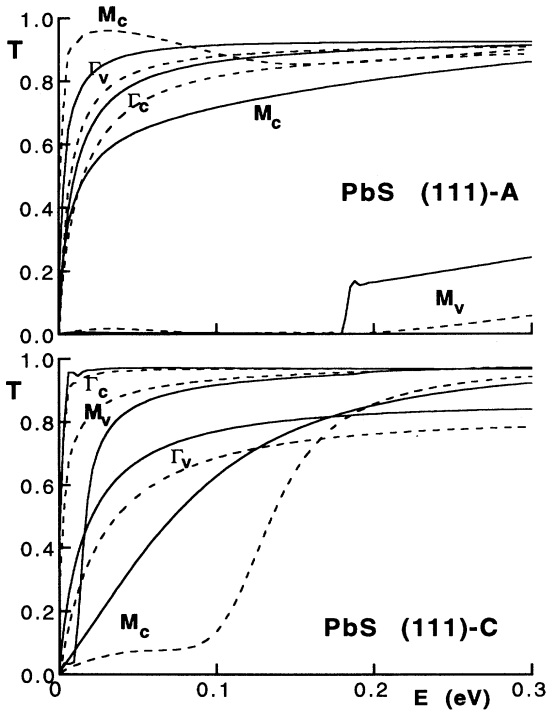

FIG. 3. The transmission coefficient vs incident electron (hole) energy for the twin boundary with anionic (A) or cationic (C) interface, calculated at $\bar{\Gamma}$ and $\bar{M}$ interface Brillouin-zone points (solid lines), or close to them ($\mathbf{k}_{\parallel}=0.05\times 2\pi/a$ off $\bar{\Gamma}$ or $\bar{M}$, dashed lines). In all cases energy is measured from the *local* band edge (for the corresponding $\mathbf{k}_{\parallel}$ value) upwards for electrons (subscript c) and downwards for holes (subscript v).

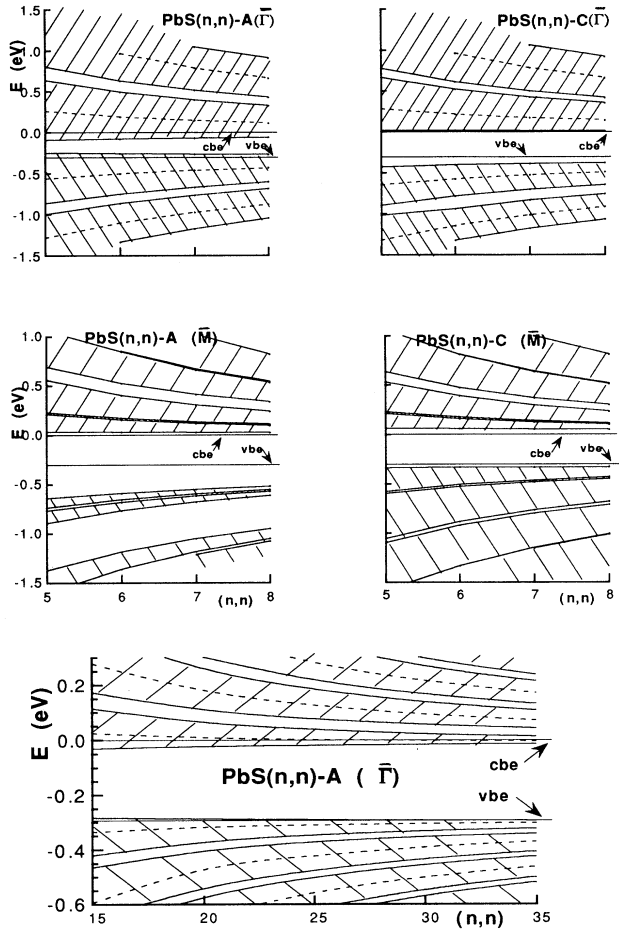

FIG. 4. Allowed minibands (cross-hatched) in PbS-based (n,n) symmetric twinning superlattices with anionic (A) and cationic (C) interfaces, calculated at $\bar{\Gamma}$ and $\bar{M}$ points of the interface Brillouin zone. Energy is measured from the conduction-band edge. At the $\bar{\Gamma}$ point there is zero-energy gap between any two neighboring minibands corresponding to $k_{SL}d=\pi$, where k_{SL} and d denote the superlattice wave vector and period, respectively. These common miniband edges are denoted by dashed lines, while miniband edges separated by finite gaps (corresponding to $k_{SL}d=0$) are denoted by solid lines. At the $\bar{M}$ point, due to the spin-orbit interaction, finite gaps separate all the minibands. The top four figures are for short-period superlattices, and the bottom one is for the long-period case (type A and at the $\bar{\Gamma}$ point only).

anionic interfaces interact strongly when a superlattice is formed. This creates envanescent-like broad minibands outside both the conduction and the valence bands, resulting in a substantial *reduction* of the band gap. As the superlattice period increases, these evanescent state minibands eventually collapse into corresponding interface states. However, very long periods are required for this to happen (Fig. 4, bottom). In the case of cationic interfaces it is only the scattering that determines the miniband energies, and the band gap is somewhat enhanced over the bulk value. As the superlattice period increases beyond $n\geq 20$ or so, the width of minibands becomes much narrower (tens or hundreds of meV), typical for conventional superlattices. This feature, and the absence of any oscillations of miniband energies as the period increases, make the PbS twinning superlattices quite different from those based on zinc-blende-type semiconductors.[7]

Since the mechanisms of twin generation are not exactly known and controllable, the realization of PbS twinning superlattices is not presently achievable. It is possible that this can be done in a way similar to that described in Ref. 12 for single twins in silicon. Also very interesting are the naturally occurring short-period (113) twinning superlattices in the alloy PbS-Bi_2S_3 (e.g., Ref. 13), for which the results qualitatively similar to those obtained here (Fig. 4) may be expected. However, these superlattices will be separately studied in a future publication.

In summary, we have studied the electronic properties of twin boundaries and twinning superlattices in PbS, and found substantial difference from those of bulk PbS, which may lead to their interesting electronic and optical properties.

The authors would like to thank the EPSRC (U.K.) for computational facilities through the CSI scheme. One of the authors (Z.I.) is grateful to the EPSRC (U.K.) for financial support.

[1]J. P. Stark, Phys. Rev. B **38**, 1139 (1988).
[2]R. W. Cahn, Adv. Phys. **3**, 202 (1954).
[3]S. V. Nistor, J. Mater. Sci. **18**, 1625 (1983).
[4]J. M. Garcia-Ruiz, J. Cryst. Growth **75**, 441 (1986).
[5]These data are cited as unpublished and private communication from R. Betzold, in A. Marchetti, Phys. Rev. B **50**, 12 164 (1994).
[6]Z. Ikonic, G. P. Srivastava, and J. C. Inkson, Solid State Commun. **86**, 799 (1993).
[7]Z. Ikonic, G. P. Srivastava, and J. C. Inkson, Phys. Rev. B **48**, 17 181 (1993).
[8]D. Y. K. Ko and J. C. Inkson, Phys. Rev. B **38**, 9945 (1988).
[9]Z. Ikonic, G. P. Srivastava, and J. C. Inkson, Phys. Rev. B **46**, 15 150 (1992).
[10]S. E. Kohn, P. Y. Yu, Y. Petroff, Y. R. Shen, Y. Tsang, and M. L. Cohen, Phys. Rev. B **8**, 1477 (1973).
[11]D. L. Mitchell and R. F. Wallis, Phys. Rev. **151**, 581 (1966).
[12]R. L. Headrick, B. E. Weir, J. Bevk, B. S. Freer, D. J. Eaglesham, and L. C. Feldman, Phys. Rev. Lett. **65**, 1128 (1990).
[13]R. J. D. Tilley and A. C. Wright, Chem. Scr. **19**, 18 (1982).

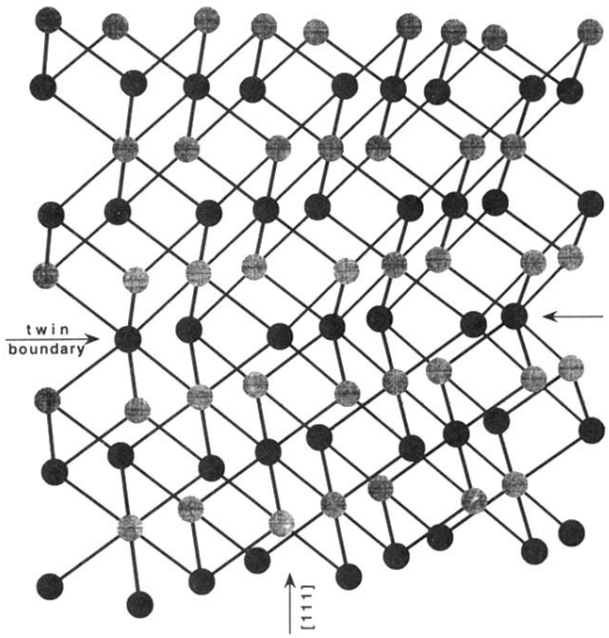

FIG. 1. The structure of PbS crystal in the vicinity of a twin boundary. Light and dark atoms may denote either of Pb and S atoms.